Copyright © 2014 Tech Science Press CMES, vol.103, no.2, pp.111-137, 2014

Construction of an Edge Finite Element Space and a Contribution to the Mesh Selection in the Approximation of the Second Order Time Harmonic Maxwell System

J. E. Sebold[1], L. A. Lacerda[2] and J. A. M. Carrer[3]

Abstract: This work is concerned with the development of the so-called Whitney and Nédélec edge finite element method for the solution of the time-harmonic Maxwell equations. Initially, the second order time harmonic Maxwell systems, as well as their variational formulation, are presented. In the sequence, Whitney and Nédélec element spaces, whose functions present continuous tangential components along the interface are built of adjacent elements. Then, numerical experiments validate the performance of Whitney and Nédélec first order elements in a two-dimensional domain. The discrete dispersion relation for the elements shows that the numerical phase velocity can be used as an error estimator. Consequently, it becomes possible to define an initial parameter to the mesh refinement that, by its turn, can make the phase difference negligible.

Keywords: Numerical Methods in Engineering, Finite elements, Maxwell equations, Wave Propagation, Computational Electromagnetism.

1 Introduction

In a numerical formulation, if one needs to directly represent a vector quantity in a discretized form, the alternative when using nodal basis functions is the separate treatment of each component of the vector field, which individually reduces to scalar functions.

Arises from this fact a dificulty related with the continuity of the discretized vector quantity across adjacent elements in the finite element mesh. For instance, in a common side of adjacent elements, nodes are shared and since the approximation is performed component by component, this approach results in continuity of all components of the vector quantity across the elements. However, if each element

[1] Federal Institute of Education, Science and Technology - Campus Araquari, Santa Catarina, Brazil.
[2] Institute of Technology for Development, Curitiba, Paraná, Brazil.
[3] Federal University of Paraná, Curitiba, Paraná, Brazil.

belongs to a different material domain, the imposed continuity produces a fisically incorrect solution. Such solutions are obtained since the nodal basis functions approach do not guarantee the continuity of the interpolation function derivatives between adjacent elements.

Along time, novel approaches were conceived to overcome this problem. Among them, one may highlight the development of techniques characterized by the use of another variety of finite elements as an alternative to the original nodal approach. Such alternatives were introduced in the works of Whitney (1957) and Nédélec (1980).

Despite using edge vectors sets in a completely different context to the finite element method developed in this work, Whitney pioneered the use of polynomials vector space to generate such sets Monk (2003b). These edge vectors or zero order elements in the context of the finite element method are an approximation by function with constant tangential components at the element edges. Such type of elements are commonly referred in the literature as Whitney elements.

Later on, Jean-Claude Nédélec presented some families of nonconforming finite elements in $\mathbb{R}^3$. In fact, it will be shown that one of these families constitute conforming elements in $H(\mathbf{curl},\Omega) = \{\boldsymbol{u} \in (L_2(\Omega))^2; \nabla \times \boldsymbol{u} \in (L_2(\Omega))^2\}$. The use of these elements in the approximation fo Maxwell and Elasticity equations were presented in Nédélec (1980). This innovative variety of finite element is knowns as vector finite element or Nédélec element.

The Sobolev spaces $H(\mathbf{curl},\Omega)$ play a central role in the variational theory of Maxwell's equations since, according to Monk (2003b) this space corresponds to the space of finite energy solutions. In this sense, it can be guaranteed the existence, uniqueness and regularity of physically significant discrete solutions Greenleaf et al. (2007). Thus, it is convenient to take this finite element space to retrieve a subspace class of suitable finite elements for the Maxwell's equations system.

Another feature of this space is the choice of the finite element discretization, which is necessary for the continuity of the tangential components of the field E across adjacent elements. Moreover, there is no obligation for the normal vector components being continuous.

Vectorial finite elements can be used in complex geometries and also in the presence of discontinuous electromagnetic properties. In the case of Maxwell's equations, the electric permittivity ε may be discontinuous across the surface of a domain Ω of $\mathbb{R}^3$, but the tangential component of the electric field $\boldsymbol{E}$ is continuous across this surface, thus it is necessary that the tangential component of the approximation field $\boldsymbol{E}_h$ is also continuous. Choosing the Nédélec elements which guarantees an approximation $H(\mathbf{curl})$-conforming, it can be seen that the tangen-

tial component of the field approximation $\boldsymbol{E}_h$ is continuous on the surface, even in the case where two adjacent elementsin the mesh have different material properties. In addition, edge finite elements have many interesting and challenging mathematical properties Monk (2003b); Ainsworth (2003); Jin (2002); Monk (2003a).

Another relevant issue is the dispersion relation for the edge finite elements. Several authors have considered the dispersive behaviour of the finite element method. Christon (1999) considered the dispersive behaviour of a variety of finite element methods for the wave equation, presenting numerical comparisons of the discrete phase and group velocities with exact values. Monk and Parrot (1994) considered the dispersive behaviour of fisrt order triangular finite elements for Maxwell's equations, while refining meshes. Monk and Cohen (1998) conducted a dispersion analysis for Nédélec type elements for time dependent Maxwell's equations using a mass matrix lumping on tensor products in two and three dimensional meshes. Ihlenburg and Babuška (1997) studied the dispersive properties of higher order finite elements for the Helmholtz equation in one dimension, obtaining estimates for the approximation to the fifth order in which $\omega h < 1$. Numerical evidences led to the conjecture that elements of order p provide an approximation of order $2p$ in dispersion relation when the mesh size parameter h tends to zero. Monk (2003a) showed proof of convergence of the Nédélec finite elements applied to a cavity problem with Maxwell's equations.The cavity was assumed to be a Lipschitz polyhedron, modelled with a rectangular non-uniform mesh. Ainsworth (2003) demonstrated that the numerical dispersion relation displays three different behaviours depending on the order of the method in relation to the mesh parameter and to the wave number. These behaviours are described as: Oscillation Phase, Transition Zone and Super-Exponential Decay. Ainsworth and Coyle (2001) studied a hierarchical basis functions set for the Galerkin discretization of $H(\mathbf{curl},\Omega)$ space for both hybrid meshes containing quadrilaterals and triangles with a non-uniform arbitrary polynomial order.

In this work, it is shown a second order time-harmonic Maxwell system problem with its approximation with edge finite elements. From the numerical results a dispersion relation analysis is performed using the numerical phase velocity, allowing the selection of an edge size parameter for a uniform quadratic elements mesh.

2 Surface Differential Operators

2.1 Surface Cross Product

Let $\boldsymbol{u} = (u_1(x,y), u_2(x,y))$ e $\boldsymbol{v} = (v_1(x,y), v_2(x,y))$ be vectors in a surface S. Surface cross product it is defined by

$$\boldsymbol{u} \times \boldsymbol{v} = u_2(x,y)v_1(x,y) - u_1(x,y)v_2(x,y) \tag{1}$$

This definition is motivated by the fact that, given two vectors $\boldsymbol{u},\boldsymbol{v} \in \mathbb{R}^3$ such that $\boldsymbol{u} = (u_1,u_2,0)$ and $\boldsymbol{v} = (v_1,v_2,0)$, one has

$$\boldsymbol{u} \times \boldsymbol{v} = (u_2v_1 - u_1v_2)\boldsymbol{k}, \tag{2}$$

where $\boldsymbol{k}$ is the unit vector in the direction of the z axis.

2.2 Surface Gradient

Let S be a surface with smooth boundary and unit normal vector $\boldsymbol{n}$. For a scalar function $\phi \in H^1(S)$ the surface gradient $\nabla_S\phi \in L_t^2(S)$ is defined as:

$$\nabla_S\phi = (\boldsymbol{n} \times \nabla\phi) \times \boldsymbol{n} \tag{3}$$

where $L_t^2(S) = \{\boldsymbol{u} = (u_1(x_1,x_2),u_2(x_1,x_2)) \in (L^2(S))^2;\ \boldsymbol{n}\cdot\boldsymbol{u} = 0 \text{ on } S\}$.

2.3 Surface Scalar Rotational

One can denote the surface scalar rotational by $\nabla_S\times : L_t^2(S) \longrightarrow H^1(S)'$, where $H^1(S)'$ is the dual of $H^1(S)$, i.e., if $g \in H^1(S)'$, then $g : H^1(S) \longrightarrow \mathbb{R}$. Thus, if $\boldsymbol{u} \in L_t^2(S)$, the surface scalar rotational according to Boffi and Perugia (1999), is given by:

$$\nabla_S \times \boldsymbol{u} = \frac{\partial u_2}{\partial x_1} - \frac{\partial u_1}{\partial x_2}, \qquad \forall\ \boldsymbol{u} \in L_t^2(S) \tag{4}$$

2.4 Surface Vector Rotational

If S denotes a Lipschitz domain in the plane xy, Reddy (1986), then for a given scalar function $\phi = \phi(x,y)$, defined on S, one can denote and define the suface vector rotational, respectively, by:

$$\nabla_S\times : H^1(S) \longrightarrow L_t^2(S) \tag{5}$$

and

$$\nabla_S \times \phi = \nabla_S\phi \times \boldsymbol{n} = \left(\frac{\partial\phi}{\partial y}, -\frac{\partial\phi}{\partial x}\right) \qquad \forall\ f \in H^1(S). \tag{6}$$

Note that equation (6) is nothing more than the product between the rotation matrix and the ϕ gradient.

Teorema 2.1 (Divergence Theorem, Kaplan (1970)) *: Let $\Omega \subset \mathbb{R}^2$ be a domain, with Lipschitz boundary Γ, and with $\boldsymbol{n}$ the unit outward normal vector, Reddy (1986). Let $\boldsymbol{F} \in (C^1(\bar{\Omega}))^2$ be a vectorial field. Hence,*

$$\int_\Omega \nabla_S \cdot \boldsymbol{F}\ d\Omega = \int_\Gamma \boldsymbol{F}\cdot\boldsymbol{n}\ d\Gamma \tag{7}$$

2.5 Surface Divergence

One can denote the surface divergence by the operator $\nabla_S \cdot : L_t^2(S) \longrightarrow H^1(S)'$ and define it as

$$\nabla_S \cdot \boldsymbol{v} = \nabla_S \times (\boldsymbol{n} \times \boldsymbol{v}) \quad \forall\, \boldsymbol{v} \in L_t^2(S) \tag{8}$$

Here, $(\boldsymbol{n} \times \boldsymbol{v})$ means a 90 degrees rotation of the vetor $\boldsymbol{v} = (v_1, v_2)$ on a surface, i.e., $(\boldsymbol{n} \times \boldsymbol{v}) = (-v_2, v_1)$. Furthermore, using the identity $\nabla_S \cdot (\boldsymbol{v}\phi) = \nabla_S \phi \cdot \boldsymbol{v} + \phi \nabla_S \cdot \boldsymbol{v}$ and the Theorem 2.1, the operator $\nabla_S \cdot$ satisfy the following identity:

$$\int_S \nabla_S \cdot \boldsymbol{v}\phi \; d\Omega = -\int_S \boldsymbol{v} \cdot \nabla_S \phi \; d\Omega \quad \forall\, \phi \in H^1(S) \;\text{ e }\; \forall\, \boldsymbol{v} \in L_t^2(S) \tag{9}$$

The Finite Element Method is based on the variational formulation or weak formulation of boundary value problems. Thus, the following theorem is very useful in the variational formulation of the second order time harmonic Maxwell system, which will be discussed below.

Teorema 2.2 (Two Dimensional Stokes Theorem) *Let $S \subset \mathbb{R}^2$ be a bounded Lipschitz domain and unit tangent vector $\boldsymbol{t}$ to boundary Γ. if $\boldsymbol{v} \in (C^1(\bar{S}))^2$ and $w \in C^1(\bar{S})$,then*

$$\int_S (\nabla_S \times \boldsymbol{v}) w \; d\Omega = \int_S \boldsymbol{v} \cdot \nabla_S \times w \; d\Omega + \int_\Gamma \boldsymbol{t} \cdot \boldsymbol{v} w \; d\Gamma \tag{10}$$

Proof: Given $\boldsymbol{v} = (v_1, v_2) \in (C^1(\bar{S}))^2$ e $w \in C^1(\bar{S})$. Consider also $\boldsymbol{n} = (n_1, n_2)$, unit outward normal vector. Let $\boldsymbol{u} \in (C^1(\bar{S}))^2$ be a vectorial field such that $\boldsymbol{u} = (u_1, u_2) = (wv_2, -wv_1)$. Note that $\boldsymbol{v}w = (-u_2, u_1)$. Thus, if $\boldsymbol{t} = (-n_2, n_1)$ is the vetor unit tangent vector to $\boldsymbol{n} = (n_1, n_2)$, then $\boldsymbol{u} \cdot \boldsymbol{n} = \boldsymbol{v}w \cdot \boldsymbol{t}$. Now, using equations (4) and (6), we obtain $\nabla_S \times \boldsymbol{v} = \frac{\partial v_2}{\partial x_1} - \frac{\partial v_1}{\partial x_2}$ and $\nabla_S \times w = \left(\frac{\partial w}{\partial x_2}, -\frac{\partial w}{\partial x_1} \right)$. Therefore, $(\nabla_S \times \boldsymbol{v})w = w\frac{\partial v_2}{\partial x_1} - w\frac{\partial v_1}{\partial x_2}$ and $\boldsymbol{v} \cdot \nabla_S \times w = v_1 \frac{\partial w}{\partial x_2} - v_2 \frac{\partial w}{\partial x_1}$. Thus, $\nabla_S \cdot \boldsymbol{u} = (\nabla_S \times \boldsymbol{v})w - \boldsymbol{v} \cdot \nabla_S \times w$. Using Theorem 2.1 on $\boldsymbol{u}$, we obtain (10).

3 Second Order Time Harmonic Maxwell System

The electromagnetic field in $\mathbb{R}^3$ is characterized by four vector functions of position and time: the electric field $\mathcal{E}$, the displacement vector $\mathcal{D}$, the magnetic field $\mathcal{H}$ and the magnetic induction $\mathcal{B}$. The basic laws of the electromagnetic field are expressed by the Maxwell's equations, Jackson (1999), Soares et al. (2008), in a system with four vector functions including the density of electric charge ρ and the electric current density $\mathcal{J}$. In many systems involving electromagnetic waves the

time changes are of the cosine form and can be expressed by $e^{-i\omega_0 t}$, consequetly the time-dependent problem can be reduced to the time harmonic Maxwell system, as discussed below. If the radiation has temporal frequency ω_0, where $\omega_0 > 0$, the real part(Re) of the time harmonic fields $\tilde{\boldsymbol{E}}$, $\tilde{\boldsymbol{H}}$, $\tilde{\boldsymbol{D}}$, $\tilde{\boldsymbol{B}}$ are related to the fields $\mathcal{E}$, $\mathcal{D}$, $\mathcal{H}$ and $\mathcal{B}$, respectively, by

$$\mathcal{E}(x,y,z,t) = Re(e^{-i\omega_0 t}\tilde{\boldsymbol{E}}(x,y,z)) \tag{11}$$

$$\mathcal{H}(x,y,z,t) = Re(e^{-i\omega_0 t}\tilde{\boldsymbol{H}}(x,y,z)) \tag{12}$$

$$\mathcal{D}(x,y,z,t) = Re(e^{-i\omega_0 t}\tilde{\boldsymbol{D}}(x,y,z)) \tag{13}$$

$$\mathcal{B}(x,y,z,t) = Re(e^{-i\omega_0 t}\tilde{\boldsymbol{B}}(x,y,z)) \tag{14}$$

Note that the same relation holds for ρ and $\mathcal{J}$.

Lemma 3.1 *: If $Re(A_1 e^{-i\omega_0 t}) = Re(A_2 e^{-i\omega_0 t})$ for all t, then $A_1 = A_2$.*

Proof: Suppose $A_1 \neq A_2$. Consider that $A_1 = a + bi$ and $A_2 = c + di$, where $a,b,c,d \in \mathbb{R}$. By hypotesis $Re(A_1 e^{-i\omega_0 t}) = Re(A_2 e^{-i\omega_0 t})$ for all t, thus for $t = 0$, one has $Re(A_1) = Re(A_2)$. Consider now $t = \pi/2\omega_0$, so one has $Im(A_1) = Im(A_2)$(imaginaries parts), which contradicts the choice $A_1 \neq A_2$. Therefore, $A_1 = A_2$.

Applying the curl operator $\nabla\times$ in the equation (11), one obtains $\nabla \times \mathcal{E} = Re(\nabla_S \times e^{-i\omega_0 t}\tilde{\boldsymbol{E}})$. In particular, from Faraday's Law of electromagnetic induction it can be noted that $\nabla \times \mathcal{E} = Re(i\omega_0 e^{-i\omega_0 t}\tilde{\boldsymbol{B}})$. It follows from Lemma 3.1 that $\nabla \times \tilde{\boldsymbol{E}} = i\omega_0\tilde{\boldsymbol{B}}$. Likewise, similar conclusions can be found for the other equations (I1.a), Jackson (1999). So, the time harmonic Maxwell system can be written

$$\nabla \times \tilde{\boldsymbol{E}} = i\omega_0\tilde{\boldsymbol{B}} \tag{15}$$

$$\nabla \times \tilde{\boldsymbol{H}} = -i\omega_0\tilde{\boldsymbol{D}} + \tilde{\boldsymbol{J}} \tag{16}$$

$$\nabla \cdot \tilde{\boldsymbol{D}} = \tilde{\rho} \tag{17}$$

$$\nabla \cdot \tilde{\boldsymbol{B}} = 0 \tag{18}$$

In heterogeneous and isotropic materials, the most common in practice and where the domain of the electromagnetic field is composed of different materials, the time harmonic fields are subject to constitutive laws, Macedo (1988), linked fields $\tilde{\boldsymbol{E}}$ to $\tilde{\boldsymbol{D}}$, $\tilde{\boldsymbol{H}}$ to $\tilde{\boldsymbol{B}}$ and $\tilde{\boldsymbol{J}}$ to $\tilde{\boldsymbol{E}}$ by $\tilde{\boldsymbol{E}} = 1/\varepsilon\tilde{\boldsymbol{D}}$, $\tilde{\boldsymbol{H}} = 1/\mu\tilde{\boldsymbol{B}}$ and $\tilde{\boldsymbol{J}} = \sigma\tilde{\boldsymbol{E}} + \boldsymbol{J}_a$, where ε, μ and σ are position functions called electric permittivity, magnetic permeability and

medium conductivity, while $\boldsymbol{J}_a$ is the applied current density. In vacuum or in the air, according to Colton and Kress (1983), we can further define the time harmonic electric and magnetic fields can be further defined according to

$$\boldsymbol{E} = \varepsilon_0^{1/2}\tilde{\boldsymbol{E}} \quad \text{and} \quad \boldsymbol{H} = \mu_0^{1/2}\tilde{\boldsymbol{H}} \tag{19}$$

The relative permeability and permittivity by their turn, are respectively defined as $\varepsilon_r = 1/\varepsilon_0(\varepsilon + (i\sigma/\omega_0))$ and $\mu_r = \mu/\mu_0$. After substituting the constitutive relation $\tilde{\boldsymbol{H}} = 1/\mu\tilde{\boldsymbol{B}}$ in (15), the constitutives relations $\tilde{\boldsymbol{J}} = \sigma\tilde{\boldsymbol{E}} + \boldsymbol{J}_a$ and $\tilde{\boldsymbol{E}} = 1/\varepsilon\tilde{\boldsymbol{D}}$ in (16) and using (19), the first order time harmonic Maxwell system obtained; it is written as:

$$\begin{cases} \nabla \times \boldsymbol{E} - i\omega_0\sqrt{\varepsilon_0\mu_0}\mu_r\boldsymbol{H} = \boldsymbol{0} \\ -i\varepsilon_r\omega_0\sqrt{\varepsilon_0\mu_0}\boldsymbol{E} - \nabla \times \boldsymbol{H} = -\boldsymbol{J}_a\mu_0^{1/2} \end{cases} \tag{20}$$

Eliminating $\boldsymbol{H}$ in (20), and then multiplying the resulting expression by $-i\mu_r\sqrt{\varepsilon_0\mu_0}$ the second order time harmonic Maxwell system is obtained:

$$-\omega^2\varepsilon_r\boldsymbol{E} + \nabla \times \mu_r^{-1}\nabla \times \boldsymbol{E} = \boldsymbol{F} \tag{21}$$

where $\omega = \omega_0\sqrt{\varepsilon_0\mu_0}$ and $\boldsymbol{F} = i\kappa\mu_0^{1/2}\boldsymbol{J}_a$. Note that equation (21) is consistent with the surface differential operator (4) and (6), i.e.,

$$-\omega^2\varepsilon_r\boldsymbol{E} + \nabla_S \times \mu_r^{-1}\nabla_S \times \boldsymbol{E} = \boldsymbol{F} \tag{22}$$

4 Description of Edge Finite Elements Space

This section discuss the discretization of time harmonic Mawell system. Let $\mathcal{M}$ be a partition of Ω in quadrilaterals such that the non-empty intersection between different elements is either an edge or a vertex. Each element $K \in \mathcal{M}$ is the image of a reference element $\hat{K} = (-1.1)^2$ via a differentiable bijection $\boldsymbol{F}_K : \hat{K} \longrightarrow K$. A finite element, according with Ciarlet (1978), is represented by a triple $(K, \mathcal{P}, \Sigma)$ where K represents the geometry of the element(a quadrilateral for instance), $\mathcal{P}$ represents spaces of functions defined over K, usually a polynomial, and Σ is a set of linear functionals on $\mathcal{P}$. On the other hand, the finite element reference is the triple $(\hat{K}, \hat{\mathcal{P}}, \hat{\Sigma})$, where $\hat{K}$ is the the domain of $\boldsymbol{F}_K$ geometry, $\hat{\mathcal{P}}$ is a space of functions defined on $\hat{K}$, usually a space of polynomials, and $\hat{\Sigma}$ is a set of linear functionals on $\hat{\mathcal{P}}$.

4.1 Degree of Freedom

An element $\alpha \in \Sigma$ (or $\hat{\Sigma}$) is called degree of freedom. A degree of freedom is generally associated with some geometric entity of K (or $\hat{K}$) as a vertex or an edge (see figure 1(a) and 1(b)).

It is said that the finite element $(K,\mathcal{P},\Sigma)$ is unisolvent if $\forall\ \boldsymbol{p}\in\mathcal{P},\ \ \alpha(\boldsymbol{p})=0,\ \ \forall\ \alpha\in\Sigma$, which implies that $\boldsymbol{p}\equiv\mathbf{0}$. In addition, a finite element is said to be $H(\mathbf{curl},\Omega)$-conforming if to any $\alpha\in\Sigma$ defined only over the edge γ, $\alpha(\boldsymbol{p})=0,\forall\ \boldsymbol{p}\in\mathcal{P}$, which now implies $\boldsymbol{n}\times\boldsymbol{p}=0$ on the edge γ. In other words, if $\boldsymbol{p}_1,\boldsymbol{p}_2\in\mathcal{P}$ are, respectively, interpolants of the geometric elements K_1 and K_2 that share the same edge, then $\boldsymbol{p}_1$ and $\boldsymbol{p}_2$ has the same tangential components.

One way to ensure continuity between two elements with the same interface, is to consider the degrees of freedom on an edge $\boldsymbol{\gamma}$ as the weighting moments of the tangential component of a field $\hat{\boldsymbol{E}}\in\mathbb{E}_p$, where

$$\mathbb{E}_p=\left\{\hat{\boldsymbol{E}}=(\hat{E_1},\hat{E_2});\ E_1=span\{\mathbb{S}_{p,p+1}\}\ \text{ e }\ E_2=span\{\mathbb{S}_{p+1,p}\}\right\} \tag{23}$$

where $\mathbb{S}_{p,q}$ represents the monomials set of degree less than or equal to p in $\hat{x}$ and of degree less than or equal to q in $\hat{y}$, i.e. $\mathbb{S}_{p,q}=\{\hat{x}^i\hat{y}^j:\ 0\le i\le p;\ 0\le j\le q\}$. The degrees of freedom at the edges of the reference element are defined the by linear functional $\alpha_\gamma\in\hat{\mathcal{P}}'$

$$\alpha_\gamma(\boldsymbol{u})=\int_{\boldsymbol{\gamma}}(\boldsymbol{t}\cdot\boldsymbol{u})\phi\ ds\quad\ \forall\ \phi\in\mathbb{P}_{k-1}(\boldsymbol{\gamma})\qquad k=1,...,p+1 \tag{24}$$

where $\boldsymbol{t}$ is the unit tangent vector to the edge, $\hat{\mathcal{P}}'$ denotes the dual space $\hat{\mathcal{P}}$ and $\mathbb{P}_{k-1}$ represents the polynomials space with degree less or equal to $k-1$. The edges have a total of $4(p+1)$ degrees of freedom. Degrees of freedom within the reference element are defined by the linear functional $\alpha_{int}\in\hat{\mathcal{P}}'$

$$\alpha_{int}(\boldsymbol{u})=\int_{\hat{K}}(\boldsymbol{u}\cdot\boldsymbol{\phi})\ d\hat{K}\quad\ \forall\ \boldsymbol{\phi}=\begin{bmatrix}\phi_1\\ \phi_2\end{bmatrix} \tag{25}$$

where $\phi_1\in\mathbb{S}_{k-2,k-1}$ and $\phi_2\in\mathbb{S}_{k-1,k-2}$. One has a total of $2p(p+1)$ degrees of freedom within the reference element $\hat{K}$.

An edge finite element $(\mathcal{P},K,\Sigma)$ on the physical domain K is built from the reference element $(\hat{\mathcal{P}},\hat{K},\hat{\Sigma})$ as follows: Let $\boldsymbol{E}=(E_1,E_2)$ be a vector field. The m^{th} degree of freedom on the edge γ is given by the linear mapping

$$\boldsymbol{E}\longrightarrow\int_\gamma v_m\boldsymbol{E}\cdot d\boldsymbol{x},$$

where the weighting function v_m is chosen to coincide with the m^{th} Legendre polynomial, $L_m(t)$, when the edge γ is parametrized by $t\in(-1,1)$. In particular, let γ be an oriented edge of an element in the mesh with endpoints $\boldsymbol{x}_{v_a}$ e $\boldsymbol{x}_{v_b}$, where the indices v_a e v_b correspond to adjacent vertices in the quadrilateral element. Now, the parameterization on the edge can be presents as follows:

$$\boldsymbol{x}(t)=(x(t),y(t))=\frac{1}{2}(1-t)\boldsymbol{x}_{v_a}+\frac{1}{2}(1+t)\boldsymbol{x}_{v_b}\qquad\text{with}\qquad t\in(-1,1) \tag{26}$$

Hence, according to Kaplan (1970), one has

$$\int_{\gamma} v_m \boldsymbol{E} \cdot d\boldsymbol{x} = \int_{-1}^{1} L_m(t) \left(E_1 \frac{dx}{dt} + E_2 \frac{dy}{dt} \right) dt = \int_{-1}^{1} L_m(t) \boldsymbol{E} \cdot \boldsymbol{\chi}_{\gamma} dt, \tag{27}$$

where $\boldsymbol{\chi}_{\gamma} = (\frac{dx}{dt}, \frac{dy}{dt})$ is the tangent vector on the edge γ.

Let F_K be a mapping of the reference element to the physical element K, $F_K : \hat{K} \longrightarrow K$, defined by

$$F_K(\hat{\boldsymbol{x}}) = J_K \hat{\boldsymbol{x}} + \boldsymbol{b}, \tag{28}$$

where J_K is an invertible square matrix and $\boldsymbol{b}$ is a translation vector. Note that F_K is a differentiable bijection, and that the Jacobian matrix transformation is given by $dF_K = J_K$. It comes from the covariant transformation, Kaplan (1970), that the tangent vectors $\boldsymbol{\chi}$ and $\boldsymbol{\tau}$ are related by

$$\boldsymbol{\chi}(\boldsymbol{x}) = J_K(\hat{\boldsymbol{x}}) \boldsymbol{\tau}(\boldsymbol{\kappa})$$

Therefore, equation (27) can be represent by:

$$\int_{-1}^{1} L_m(t) \boldsymbol{E} \cdot (J_K \boldsymbol{\tau}) dt$$

By using the mapping F_{γ}, restricted to reference edge γ and with $m = k$, one has

$$\int_{-1}^{1} L_k(t) \boldsymbol{E} \cdot (J_K \boldsymbol{\tau}) dt = \int_{-1}^{1} L_k(s) J_K^T \boldsymbol{E} \cdot \boldsymbol{\tau} ds$$

Note that the electric field $\hat{\boldsymbol{E}}$ on a reference element $\hat{K}$ is related to the electric field $\boldsymbol{E}$, defined on physical element K by the covariant transformation, Kaplan (1970)

$$\boldsymbol{E}(\boldsymbol{x})|_K = J_K^{-T} \hat{\boldsymbol{E}}(\hat{\boldsymbol{x}}), \qquad \boldsymbol{x} = \boldsymbol{F}_K(\hat{\boldsymbol{x}}). \tag{29}$$

Similarly, the global basis function $\boldsymbol{\phi}_{i,j}$, corresponding to the local basis function $\hat{\boldsymbol{\phi}}_{i,j}$ on the reference element, is defined by

$$\boldsymbol{\phi}_{i,j}(\boldsymbol{x})|_K = J_K^{-T} \hat{\boldsymbol{\phi}}_{i,j}(\hat{\boldsymbol{x}}), \qquad \boldsymbol{x} = \boldsymbol{F}_K(\hat{\boldsymbol{x}}). \tag{30}$$

The degrees of freedom on the edges ensures that $(K, \mathcal{P}, \Sigma)$ is $H(\mathbf{curl}, \Omega)$-conforming; complementing them with the degrees of freedom inside of element, it is ensured that $(K, \mathcal{P}, \Sigma)$ is unisolvente (see Theorem 5 of Nédélec (1986)).

4.2 Hierarchical Basis Functions

Let $\hat{\mathcal{P}} = \mathbb{E}_p$ be the space of polynomials associated with the edge finite element of order p on the reference element $\hat{K}$. Let $\{L_k\}_{k=0}^{p}$ be the Legendre orthogonal polynomials set, which are given by the Rodrigues formula, Olver et al. (2010), Zhang et al. (2014),

$$L_k(\kappa) = \frac{1}{2^k k!}\frac{d^{(k)}}{d\kappa^k}\left[(\kappa^2-1)^k\right] \qquad 0 \le k \le p \tag{31}$$

Furthermore, the set $\{l_k\}_{k=0}^{p+1}$ is defined as follows:

$$\begin{cases} l_k(\kappa) = \dfrac{1}{2}(1+\xi_k\kappa), & k = 0,1, \\ l_k(\kappa) = \frac{1}{||L_{k-2}||}\int_{-1}^{\kappa} L_{k-2}(t)\,dt, & k = 2,...,p+1 \end{cases} \tag{32}$$

where $\xi_0 = -1$, $\xi_1 = 1$ and $||L_{k-2}||^2 = \frac{2}{2k-3}$, Harari et al. (1996). Note that, by the orthogonality of Legendre polynomials, one has $l_k(-1) = l_k(1) = 0$, whenever $k > 1$. The set$\{l_k\}_{k=0}^{p+1}$ is used for setting hierarchical basis function, which are useful for adaptivefinite element methods, Adjerid (2002). Using the functions L_k and l_k, the basis functions associated to the degrees of freedom at the edges are defined as:

$$\begin{cases} \boldsymbol{\phi}^{\gamma}_{i,j,1}(\hat{\boldsymbol{x}}) = L_i(\hat{x})l_j(\hat{y})\boldsymbol{e}_1 \\ \boldsymbol{\phi}^{\gamma}_{i,j,2}(\hat{\boldsymbol{x}}) = l_j(\hat{x})L_i(\hat{y})\boldsymbol{e}_2 \end{cases} \qquad i = 0,...,p; \quad j = 0,1 \tag{33}$$

where $\boldsymbol{e}_1 = (1,0)$ and $\boldsymbol{e}_2 = (0,1)$ denote the canonical basis of $\mathbb{R}^2$ and $\hat{x}$, $\hat{y}$ are the coordinates of $\hat{\boldsymbol{x}}$. Basis functions associated with the degrees of freedom inside of an element are complementary functions on (33) when using l_k with $k \ge 2$:

$$\begin{cases} \boldsymbol{\phi}^{int}_{i,j,1}(\hat{\boldsymbol{x}}) = L_i(\hat{x})l_j(\hat{y})\boldsymbol{e}_1 \\ \boldsymbol{\phi}^{int}_{i,j,2}(\hat{\boldsymbol{x}}) = l_j(\hat{x})L_i(\hat{y})\boldsymbol{e}_2 \end{cases} \qquad i = 0,...,p; \quad j = 2,...,p+1, \tag{34}$$

Inspite of the representations (33) and (34) be well simplified, a notation to differentiate the "edges functions" were used. This classification takes into account the edges of a quadrilateral reference element:

$$\begin{aligned} &\boldsymbol{\phi}^{\gamma_1}_i(\hat{\boldsymbol{x}}) = L_i(\hat{x})l_0(\hat{y})\boldsymbol{e}_1; \quad \boldsymbol{\phi}^{\gamma_2}_i(\hat{\boldsymbol{x}}) = L_i(\hat{x})l_1(\hat{y})\boldsymbol{e}_1; \\ &\boldsymbol{\phi}^{\gamma_3}_i(\hat{\boldsymbol{x}}) = L_i(\hat{y})l_0(\hat{x})\boldsymbol{e}_2; \quad \boldsymbol{\phi}^{\gamma_4}_i(\hat{\boldsymbol{x}}) = L_i(\hat{y})l_1(\hat{x})\boldsymbol{e}_2, \end{aligned} \tag{35}$$

Thus, the basis function associated with the edges satisfy

$$\int_{\boldsymbol{\gamma}_l} (\boldsymbol{t}\cdot\boldsymbol{\phi}^{\gamma_j}_i)L_k ds = \delta_{lj}\delta_{ik}||L_i||^2 \quad \text{with} \quad j = 1,2,3,4 \tag{36}$$

where δ is the Kronecker delta. Similarly, the basis functions associated to the inside of an element satisfies

$$\begin{aligned}\int_{\hat{K}} L_m(\hat{x})l_n(\hat{y})\boldsymbol{\phi}^{int}_{i,j,1}\cdot\boldsymbol{e}_1 d\hat{x}d\hat{y} &= \delta_{mi}\delta_{nj}||L_i||^2||l_j||^2\\ \int_{\hat{K}} L_m(\hat{y})l_n(\hat{x})\boldsymbol{\phi}^{int}_{i,j,2}\cdot\boldsymbol{e}_2 d\hat{x}d\hat{y} &= \delta_{mi}\delta_{nj}||L_i||^2||l_j||^2\end{aligned} \tag{37}$$

4.3 Basis Function for Whitney Elements ($p = 0$)

An emphasis on the definition of $\mathbb{E}_p$ for the case $p = 0$, implies $\mathbb{S}_{0,1} = \{1,\hat{y}\}$ and $\mathbb{S}_{1,0} = \{1,\hat{x}\}$; therefore:

$$\mathbb{E}_0 = \left\{\hat{\boldsymbol{E}} = (\hat{E_1},\hat{E_2});\ \hat{E_1} = span\{1,\hat{y}\}\ \text{ and }\ \hat{E_2} = span\{1,\hat{x}\}\right\} \tag{38}$$

For Whitney elements each edge presents only one degree of freedom(see equation (24)), thus we can define the basis functions can be defined as:

$$\begin{aligned}&\boldsymbol{\phi}_0^{\gamma_1}(\hat{\boldsymbol{x}}) = L_0(\hat{x})l_0(\hat{y})\boldsymbol{e}_1;\quad \boldsymbol{\phi}_0^{\gamma_2}(\hat{\boldsymbol{x}}) = L_0(\hat{x})l_1(\hat{y})\boldsymbol{e}_1;\\ &\boldsymbol{\phi}_0^{\gamma_3}(\hat{\boldsymbol{x}}) = L_0(\hat{y})l_0(\hat{x})\boldsymbol{e}_2;\quad \boldsymbol{\phi}_0^{\gamma_4}(\hat{\boldsymbol{x}}) = L_0(\hat{y})l_1(\hat{x})\boldsymbol{e}_2,\end{aligned} \tag{39}$$

Zero-order functions can be characterized by the fact that they have free divergent, i.e., $\nabla_S\cdot\boldsymbol{\phi}_0^{\gamma_i} = 0$, and also for having constant tangential component on each edge $\boldsymbol{\gamma}_i$, Jin (2002). Figure 1(a) shows the degrees of freedom distributed on the edges of the reference element.

4.4 Basis Function for Nédélec Elements ($p = 1$)

The space of polynomials associated with the Nédélec elements of order $p = 1$ on the reference element $\hat{K}$ is defined as

$$\mathbb{E}_1 = \left\{\hat{\boldsymbol{E}} = (\hat{E_1},\hat{E_2});\ \hat{E_1} = span\{\mathbb{S}_{1,2}\}\ \text{ and }\ \hat{E_2} = span\{\mathbb{S}_{2,1}\}\right\}, \tag{40}$$

where

$$\mathbb{S}_{1,2} = \{1,\hat{y},\hat{y}^2,\hat{x},\hat{x}\hat{y},\hat{x}\hat{y}^2\}\ \ e\ \ \mathbb{S}_{2,1} = \{1,\hat{x},\hat{x}^2,\hat{y},\hat{y}\hat{x},\hat{y}\hat{x}^2\} \tag{41}$$

and $\mathbb{E}_1$ is constructed by increasing the space $\mathbb{E}_0$ – Hierarchical basis. Furthermore, we note that there are four new basis functions on edges that are generated by the elements $\hat{x},\hat{x}\hat{y}\in\mathbb{S}_{1,2}$ and $\hat{y},\hat{y}\hat{x}\in\mathbb{S}_{2,1}$, which will be added to the edges together with the basis functions for elements of Whitney.

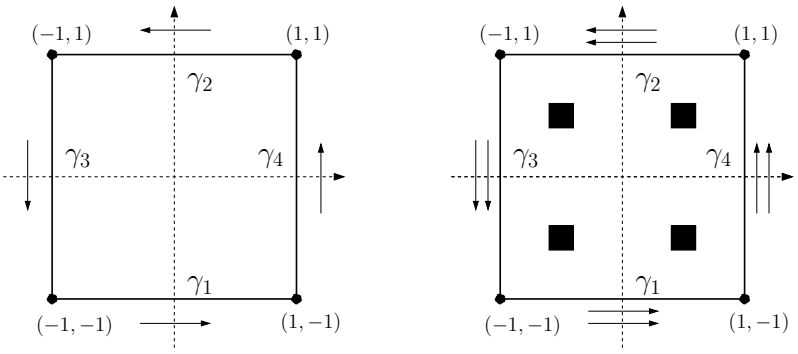

Figure 1: (a) Degrees of freedom for Whitney elements. The arrows indicate the zero-order moment of the tangential field $\hat{\boldsymbol{E}}$. Note that the direction of the tangent remains in the anti-clockwise around the element; (b) The arrows indicate the degrees of freedom of the elements of order $p = 1$ distributed on the edges. The black squares in the interior of the element represent the degrees of freedom necessary for a quadrilateral.

Unlike the basis functions for Whitney elements, here interior basis functions generated by elements $\hat{x},\hat{y}^2,\hat{x}\hat{y}^2 \in \mathbb{S}_{1,2}$ and $\hat{y},\hat{x}^2,\hat{y}\hat{x}^2 \in \mathbb{S}_{2,1}$ are also taken into account. Figure 1(b) shows the distribution of degrees of freedom on the quadrilateral element.

Note that, the elements of order $p = 1$ are provided degrees of freedom on the edges and inside the element. Thus, the basic functions of these elements are organized as follows:

1. Basis function in the edges:

$$\begin{cases} \boldsymbol{\phi}_0^{\gamma_1}(\hat{\mathbf{x}}) = L_0(\hat{x})l_0(\hat{y})\boldsymbol{e}_1; \quad \boldsymbol{\phi}_0^{\gamma_2}(\hat{\mathbf{x}}) = L_0(\hat{x})l_1(\hat{y})\boldsymbol{e}_1; \\ \boldsymbol{\phi}_0^{\gamma_3}(\hat{\mathbf{x}}) = L_0(\hat{y})l_0(\hat{x})\boldsymbol{e}_2; \quad \boldsymbol{\phi}_0^{\gamma_4}(\hat{\mathbf{x}}) = L_0(\hat{y})l_1(\hat{x})\boldsymbol{e}_2 \\ \boldsymbol{\phi}_1^{\gamma_1}(\hat{\mathbf{x}}) = L_1(\hat{x})l_0(\hat{y})\boldsymbol{e}_1; \quad \boldsymbol{\phi}_1^{\gamma_2}(\hat{\mathbf{x}}) = L_1(\hat{x})l_1(\hat{y})\boldsymbol{e}_1; \\ \boldsymbol{\phi}_1^{\gamma_3}(\hat{\mathbf{x}}) = L_1(\hat{y})l_0(\hat{x})\boldsymbol{e}_2; \quad \boldsymbol{\phi}_1^{\gamma_4}(\hat{\mathbf{x}}) = L_1(\hat{y})l_1(\hat{x})\boldsymbol{e}_2 \end{cases} \tag{42}$$

Note that the first four basis functions of the edge are the same basic functions for elements of order $p = 0$. The basis functions in (42) are built using the weight function $v_k = L_k$, satisfying (36).

2. Basis functions inside $\boldsymbol{\phi}_{i,j,1}^{int}$ and $\boldsymbol{\phi}_{i,j,2}^{int}$, with $i = 0,1$ and $j = 2$:

$$\begin{cases} \boldsymbol{\phi}_{0,2,1}^{int_x}(\hat{\boldsymbol{x}}) = L_0(\hat{x})l_2(\hat{y})\boldsymbol{e}_1; \quad \boldsymbol{\phi}_{1,2,1}^{int_x}(\hat{\boldsymbol{x}}) = L_1(\hat{x})l_2(\hat{y})\boldsymbol{e}_1; \\ \boldsymbol{\phi}_{0,2,2}^{int_y}(\hat{\boldsymbol{x}}) = L_0(\hat{y})l_2(\hat{x})\boldsymbol{e}_2; \quad \boldsymbol{\phi}_{1,2,2}^{int_y}(\hat{\boldsymbol{x}}) = L_1(\hat{y})l_2(\hat{x})\boldsymbol{e}_2 \end{cases} \tag{43}$$

Basis functions in (43) are constructed in order to satisfy (37).

5 Numerical Tests

Now, in order to illustrate the performance of Whitney-Nédélec edge finite elements, the problem of the propagation of a plane wave through of a square domain $\Omega = (0,1)^2$ with boundary Γ is analysed. Suppose Ω in the vacuum, thus $\varepsilon = \varepsilon_0$ and $\mu = \mu_0$.

Consider the electric field $\boldsymbol{E} \in H(\mathbf{curl}, \Omega)$ and the following boundary value problem

$$-\omega^2 \left(1 + \frac{i\sigma\mu\omega_0}{\omega^2}\right)\boldsymbol{E} + \nabla_S \times \nabla_S \times \boldsymbol{E} = \boldsymbol{F} \qquad \forall\, \boldsymbol{x} = (x_1, x_2) \in \Omega \tag{44}$$

$$\boldsymbol{n} \times \boldsymbol{E} = 0 \qquad \text{on } \Gamma, \tag{45}$$

where ω is a fixed frequency and $\boldsymbol{n} = (n_1, n_2)$ is the normal vector to Γ.

The Finite Element Method is based on the variational formulation or weak formulation of boundary value problems. Before starting the discretization of the second order system (44), an appropriate variational formulation must be stated, e.g. Monk (2003b); Reddy (1986); Kreyszig (1978). First, it is important to note as that Maxwell's equations involve complex functions in harmonic regime, the field must be adapted to complex spaces. For example, the inner product $(L_2(\Omega))^2$ is now defined by $(\boldsymbol{u}, \boldsymbol{v})_{L_2} = \int_\Omega \boldsymbol{u} \cdot \overline{\boldsymbol{v}}\, d\Omega$. For the variational formulation the procedure is done as follows: (a) multiply (44) by $\boldsymbol{\phi} \in H_0(\mathbf{curl}, \Omega) = \{\boldsymbol{x} \in H(\mathbf{curl}, \Omega);\ \boldsymbol{n} \times \boldsymbol{x} = 0\}$; (b) integrates on Ω the result of the multiplication; (c) apply the Theorem 2.2 choosing $w = \nabla_S \times \boldsymbol{E}$ and $\boldsymbol{v} = \boldsymbol{\phi}$. Thus,

$$-\omega^2 \left(\left(1 + \frac{i\sigma\mu\omega_0}{\omega^2}\right)\boldsymbol{E}, \boldsymbol{\phi}\right)_{L_2} + (\nabla_S \times \boldsymbol{E}, \nabla_S \times \boldsymbol{\phi})_{L_2} = (\boldsymbol{F}, \boldsymbol{\phi})_{L_2} \tag{46}$$

for all $\boldsymbol{\phi} \in H_0(\mathbf{curl}, \Omega)$. If the conductivity $\sigma > 0$ in Ω, then can be written (46) as a sesquilinear form that will be coercive $H_0(\mathbf{curl}, \Omega)$, Monk (1991). This ensures that (46) has a unique solution for any ω and $\boldsymbol{F} \in (L(\Omega))^2$. However, if $\sigma = 0$ in Ω, then (46) will have no solution to an infinite discrete set of ω values, which are called resonances. In this case, the sesquilinear form defined by the left side in (46)

will not be coercive, Monk (1991). To avoid this problem, the use of Fredholm theory to provides the conditions that will ensure the existence and uniqueness of a solution, Monk (2003b). Consequently, for any value imposed to σ a solution to (46) can be find.

Assuming $\boldsymbol{F} = \boldsymbol{0}$ the variational formulation (46) becomes the following problem: Find $\boldsymbol{E} \in H(\mathbf{curl}, \Omega)$ such that

$$(\nabla_S \times \boldsymbol{E}, \nabla_S \times \boldsymbol{\phi})_{L_2} = \omega^2 (\boldsymbol{E}, \boldsymbol{\phi})_{L_2} \quad \forall\, \boldsymbol{\phi} \in H_0(\mathbf{curl}, \Omega) \tag{47}$$

$$\boldsymbol{n} \times \boldsymbol{E} = f \qquad \text{on } \Gamma, \tag{48}$$

where $f : \Omega \longrightarrow \mathbb{C}$ is a continuous and smooth function. Choosing the function $f(\boldsymbol{x}) = n_2 \tilde{E}_1(\boldsymbol{x}) - n_1 \tilde{E}_2(\boldsymbol{x})$ in (48), where $(\tilde{E}_1, \tilde{E}_2) = (-10\pi e^{i\boldsymbol{\kappa}\cdot\boldsymbol{x}}, 10\pi e^{i\boldsymbol{\kappa}\cdot\boldsymbol{x}})$ is a plane wave propagating in the direction of the wave vector $\boldsymbol{\kappa} = 10\pi(1,1)$, and $\omega = 10\sqrt{2}\pi$, one has $\tilde{\boldsymbol{E}} = (\tilde{E}_1, \tilde{E}_2)$ the exact solution to (47)-(48).

Consider that the domain Ω is discretized by a uniform mesh of square elements of side h, Figure 2, and that uniform p-order elements are used to define the edge finite elements space $\boldsymbol{V}_{hp}$. The finite element approximation is: Find $\boldsymbol{E}_{hp} \in \boldsymbol{V}_{hp}$ such that

$$(\nabla_S \times \boldsymbol{E}_{hp}, \nabla_S \times \boldsymbol{v}_{hp})_{L_2} = \omega^2 (\boldsymbol{E}_{hp}, \boldsymbol{v}_{hp})_{L_2} \tag{49}$$

for all $\boldsymbol{v}_{hp} \in \boldsymbol{V}_{hp} \cap H_0(\mathbf{curl}, \Omega)$. Essential boundary conditions are imposed requiring that over all edges $\gamma \subset \Gamma$, one has

$$\int_\gamma (\boldsymbol{n} \times \boldsymbol{E}_{hp} - f) v \, ds = 0 \tag{50}$$

for all $v \in \mathbb{P}_p(\gamma)$, where $\mathbb{P}_p$ denotes the one-dimensional space of polynomials of degree at most equal to p in the arc length. Note that, if $\boldsymbol{t} = (n_2, -n_1)$ is the tangent vector on γ, equation (50) agree with equation (24). The approximation to $\tilde{\boldsymbol{E}}$ is carried out with Whitney elements and first order Nédélec elements. Some numerical experiments concerning the solution of the problem can seen in this section. Figures 3 and 4 highlight the approximation of the real part of the second component of the exact solution $\tilde{\boldsymbol{E}}$ to the problem (47)-(48).

6 Mesh parameter selection

In the preceedings section it could be seen that the error of approximation by finite elements may cause a phase difference and a amplitude difference with respect to the exact solution, see Figure 4(b). This effect depends not only on the mesh parameter h, but also on the temporal frequency ω, see Figures 5(a) and 5(b). This fact

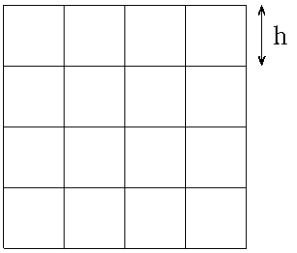

Figure 2: Example particular mesh used in the numerical experiments, with $n^2 = 16$, being n the number of elements in the base domain, i.e. $h = 1/n$.

can be analyzed through the study of the dispersive properties of numerical solution for homegeneous scalar Helmholtz equation in an infinity mesh, Ainsworth (2003). Aiming to find an expression for the discrete dispersion relation for Whitney and Nï¿½dï¿½lec Elements, one can consider some relations between the Helmholtz equation and the equation (44), with $\sigma = 0$, i.e.,

$$-\omega^2 \boldsymbol{E} + \nabla_S \times \nabla_S \times \boldsymbol{E} = \boldsymbol{0} \tag{51}$$

Dispersion relation for this equation can be described when a non-trivial plane wave solution of the kind $\boldsymbol{E}(\boldsymbol{x}) = \boldsymbol{\alpha} e^{i\boldsymbol{\kappa}\cdot\boldsymbol{x}}$ is searched for (51), where $\boldsymbol{\alpha} = (\alpha_1, \alpha_2)$. Substituting this plane wave in (51) one finds

$$(\omega^2 I + M_\kappa)\boldsymbol{\alpha} = \boldsymbol{0}, \quad \text{com} \quad M_\kappa = \begin{bmatrix} \kappa_2^2 & -\kappa_1\kappa_2 \\ -\kappa_1\kappa_2 & \kappa_1^2 \end{bmatrix} \tag{52}$$

Considering $det(\omega^2 I + M_\kappa) = 0$, the following relation arises

$$\omega = |\boldsymbol{\kappa}| \tag{53}$$

Equation (53) is the dispersion relation for (51). According to the next lemma solutions to the equation (51) can be obtained from solutions to scalar homogeneous Helmholtz equation.

Lemma 6.1 *Let $\Omega \subset \mathbb{R}^2$ be a bounded Lipschitz domain. Whenever $\phi = \phi(x_1, x_2) \in H^1(\Omega)$ present as a solution to the scalar homogeneous Helmholtz equation, the field defined by $\boldsymbol{E} = \nabla_S \times \phi$, will be a solution to the second order time harmonic Maxwell system*

$$\nabla_S \times \nabla_S \times \boldsymbol{E} = \omega^2 \boldsymbol{E} \tag{54}$$

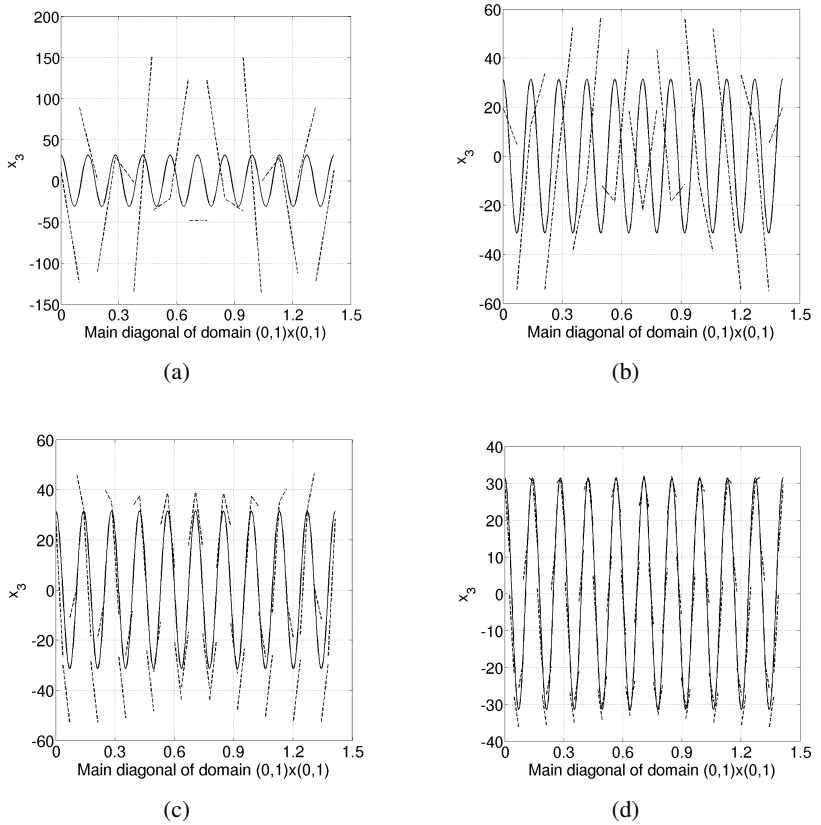

Figure 3: Variation along the main diagonal of the exact solution (continuous line) and of the numerical solution (dashed line) using Whitney elements in the levels: (a) $h = 1/15$; (b) $h = 1/20$; (c) $h = 1/40$; (d) $h = 1/60$.

Proof: Applying surface rotational twice over $\boldsymbol{E}$ we obtain $\nabla_S \times \nabla_S \times \boldsymbol{E} = \left(-\frac{\partial^3 \phi}{\partial x_2 \partial x_1^2} - \frac{\partial^3 \phi}{\partial^3 x_2^3}, \frac{\partial^3 \phi}{\partial x_1 \partial x_2^2} + \frac{\partial^3 \phi}{\partial^3 x_1^3}\right)$. Thus, one has $\nabla_S \times \nabla_S \times \boldsymbol{E} - \omega^2 \boldsymbol{E} = \boldsymbol{0}$.

Lemma 6.1 also shows that discrete solutions to (51) can be obtained from discrete solutions to the Helmholtz equation by simply taking $\boldsymbol{E}_h = \nabla_S \times \phi_h$. In fact, according to the next lemma, the components of a field $\boldsymbol{E}$ are solutions of the homogeneous scalar Helmholtz equation.

Lemma 6.2 *Let $\Omega \subset \mathbb{R}^2$ be a bounded Lipschitz domain. If $\tilde{\boldsymbol{E}}, \tilde{\boldsymbol{H}} \in H(\boldsymbol{curl}, \Omega)$ are*

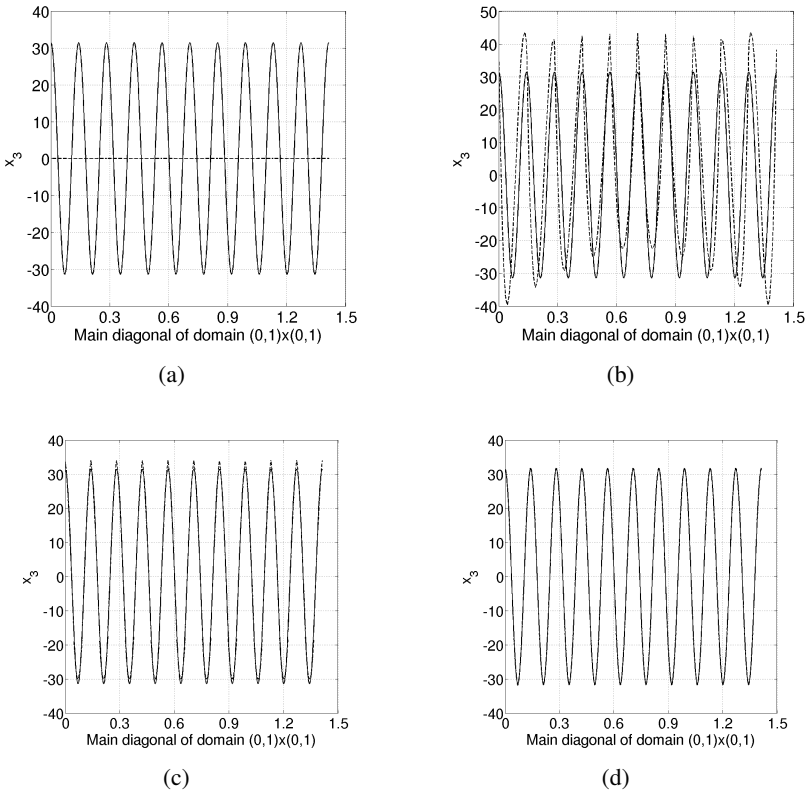

Figure 4: Variation along the main diagonal of the exact solution (continuous line) and of the numerical solution (dashed line) using first order Nédélec elements in the levels: (a) $h = 1/5$; (b) $h = 1/10$; (c) $h = 1/30$; (d) $h = 1/60$

solutions to the first-order time harmonic Maxwell system

$$\begin{cases} \nabla_S \times \boldsymbol{E} - i\kappa \boldsymbol{H} = \boldsymbol{0} \\ \nabla_S \times \boldsymbol{H} + i\kappa \boldsymbol{E} = \boldsymbol{0} \end{cases}, \tag{55}$$

then the scalar components of the field $\tilde{\boldsymbol{E}}$ and $\tilde{\boldsymbol{H}}$ are solutions to the homogeneous scalar Helmholtz equation.

Proof: Multiplying the second equation of system (55) by $i\kappa$, and then applying the surface rotational operator in the first equation of system, we can eliminate $\boldsymbol{H}$ from first equation of system to obtain $\nabla_S \times \nabla_S \times \boldsymbol{E} - \kappa^2 \boldsymbol{E} = \boldsymbol{0}$. Note that, from identities 3.33 and 3.35 in Kaplan (1970), one has, respectively, $\nabla_S \cdot \boldsymbol{E} = 0$ and

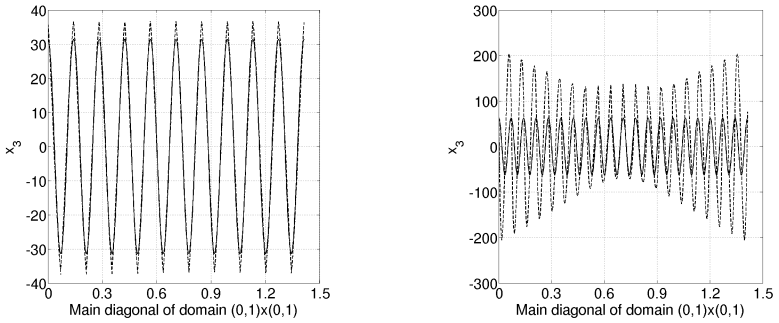

(a) (b)

Figure 5: (a) Variation along the main diagonal ($h = 1/20$) of the exact solution (continuous line) and of the numerical solution with first order Nédélec elements of the first order (dashed line) with $\omega^2 = 200\pi^2$ and with (b) $\omega^2 = 800\pi^2$.

consequently $\nabla_S \times \nabla_S \times \boldsymbol{E} - \kappa^2 \boldsymbol{E} = \nabla^2 \boldsymbol{E} + \kappa^2 \boldsymbol{E}$. Analogously is shown the same for the field $\boldsymbol{H}$.

From Lemmas 6.1 and 6.2, it is evident the correlation between Helmholtz equation and second order time harmonic Maxwell system. Thus, the expression for the discrete dispersion relation for scalar Helmholtz equation in one dimension can be used to determine an expression for the discrete dispersion relation for Whitney elements and Nédélec first order elements. In fact, as an example, consider $\boldsymbol{V}_{h0}$ as the Whitney elements space built on a uniform mesh(see Figure 2). The components of the vector function $\boldsymbol{E}_h = (E_h^{(1)}, E_h^{(2)}) \in \boldsymbol{V}_{h0}$ will be expanded in the form

$$E_h^{(d)} = \sum_{\boldsymbol{n} \in \mathbb{Z}^2} \alpha_{\boldsymbol{n}}^{(d)} \boldsymbol{\phi}_{\boldsymbol{n}}^{(d)}, \qquad d = 1,2 \qquad \boldsymbol{n} = (n_1, n_2) \tag{56}$$

where $\mathbb{Z}$ is the integer set and

$$\boldsymbol{\phi}_{\boldsymbol{n}}^{(1)} = \begin{bmatrix} \psi_{n_1}(x_1)\theta_{n_2}(x_2) \\ 0 \end{bmatrix}; \qquad \boldsymbol{\phi}_{\boldsymbol{n}}^{(2)} = \begin{bmatrix} 0 \\ \theta_{n_1}(x_1)\psi_{n_2}(x_2) \end{bmatrix} \tag{57}$$

Here, ψ_n is the characteristic function for the interval $(nh, nh+h)$, given by $\psi_n(s) = 1$ if $s \in (nh, nh+h)$ and zero otherwise, when θ_n is the piecewise continuous linear interpolation function. For $n = m-1, m, m+1$, θ_n functions as well as their

derivatives, θ_n', are defined by

$$\theta_{m-1}(s)=\begin{cases} 2-m+\dfrac{s}{h} & \text{if } s\in(mh-2h,mh-h] \\ m-\dfrac{s}{h} & \text{if } s\in(mh-h,mh) \\ 0 & \text{otherwise} \end{cases} \qquad \theta_{m-1}'(s)=\begin{cases} \dfrac{1}{h} & \text{if } s\in(mh-2h,mh-h] \\ \dfrac{-1}{h} & \text{if } s\in(mh-h,mh) \\ 0 & \text{otherwise} \end{cases}$$

$$\theta_{m}(s)=\begin{cases} 1-\left(m-\dfrac{s}{h}\right) & \text{if } s\in(mh-h,mh] \\ 1+\left(m-\dfrac{s}{h}\right) & \text{if } s\in(mh,mh+h) \\ 0 & \text{otherwise} \end{cases} \qquad \theta_{m}'(s)=\begin{cases} \dfrac{1}{h} & \text{if } s\in(mh-h,mh] \\ \dfrac{-1}{h} & \text{if } s\in(mh,mh+h) \\ 0 & \text{otherwise} \end{cases}$$

$$\theta_{m+1}(s)=\begin{cases} -m+\dfrac{s}{h} & \text{if } s\in(mh,mh+h] \\ 2+m-\dfrac{s}{h} & \text{if } s\in(mh+h,mh+2h) \\ 0 & \text{otherwise} \end{cases} \quad \theta_{m+1}'(s)=\begin{cases} \dfrac{1}{h} & \text{if } s\in(mh,mh+h] \\ \dfrac{-1}{h} & \text{if } s\in(mh+h,mh+2h) \\ 0 & \text{otherwise} \end{cases}$$

It is noteworthy that the basis functions used in this section are different from the basic functions used in Section 4. The reason for this change is that the θ_n functions are interpolants simplifying and so facilitate the dispersion analysis. However, the spaces generated by the two basis is the same.

The line integral of a basis function, $\boldsymbol{\phi}_{\boldsymbol{n}}^{(d)} \in \boldsymbol{V}_{h0}$, taken along edges of a square element, has the form

$$\int_{\gamma_{\boldsymbol{m}}^{(a)}} \boldsymbol{\phi}_{\boldsymbol{n}}^{(d)} \cdot \, d\boldsymbol{x} = \begin{cases} h & \text{if} \quad \boldsymbol{m}=\boldsymbol{n} \text{ and } d=a \\ 0 & \text{otherwise} \end{cases}, \tag{58}$$

where $\gamma_{\boldsymbol{m}}^{(a)}$ denotes the edge aligned with the a^{th} coordinate axis starting at the indexed vertex by $\boldsymbol{m}$. From equation (58), one can calculate the coefficients of $\boldsymbol{E}_h$ in (56) as follows: Multiply (58) by $\alpha_{\boldsymbol{n}}^{(a)}$ and consider $\boldsymbol{n}=\boldsymbol{m}$ and $a=d$; then:

$$\alpha_{\boldsymbol{n}}^{(a)} = \frac{1}{h}\int_{\gamma_{\boldsymbol{n}}^{(a)}} \alpha_{\boldsymbol{n}}^{(a)} \boldsymbol{\phi}_{\boldsymbol{n}}^{(a)} \cdot \, d\boldsymbol{x}$$

Using equation (56) in the d^{th} spatial component, the following expression arises:

$$\alpha_{\boldsymbol{n}}^{(a)} = \frac{1}{h}\int_{\gamma_{\boldsymbol{n}}^{(a)}} \boldsymbol{E}_h \cdot \, d\boldsymbol{x} \tag{59}$$

Furthermore, consider that a non-trivial discrete solution $\boldsymbol{E}_h$ satisfies the condition

$$\boldsymbol{E}_h(\boldsymbol{x}+h\boldsymbol{n}) = e^{ih\boldsymbol{\kappa}_h\cdot\boldsymbol{n}}\boldsymbol{E}_h(\boldsymbol{x}), \tag{60}$$

where $\boldsymbol{\kappa}_h = (\kappa_1, \kappa_2)$ is the discrete wave vector related to a prescribed temporal frequency ω through of the discrete relation dispersion. Applying a variable change in (59) and considering translation invariance of the mesh, equation (60), one has

$$\alpha_{\boldsymbol{n}}^{(d)} = \frac{1}{h}\int_{\gamma_{\boldsymbol{n}}^{(d)}} \boldsymbol{E}_h(\boldsymbol{x})\cdot\, d\boldsymbol{x} = \frac{1}{h}\int_{\gamma_{\boldsymbol{0}}^{(d)}} e^{ih\boldsymbol{\kappa}_h\cdot\boldsymbol{n}}\boldsymbol{E}_h(\boldsymbol{y})\cdot\, d\boldsymbol{y} \tag{61}$$

consequently,

$$\alpha_{\boldsymbol{n}}^{(d)} = e^{ih\boldsymbol{\kappa}_h\cdot\boldsymbol{n}}\alpha_{\boldsymbol{0}}^{(d)} \qquad \forall \boldsymbol{n}\in\mathbb{Z}^2 \tag{62}$$

Replacing equation (62) in (56), one finds

$$E_h^{(d)} = \alpha_{\boldsymbol{0}}^{(d)}\sum_{\boldsymbol{n}\in\mathbb{Z}^2} e^{ih\boldsymbol{\kappa}_h\cdot\boldsymbol{n}}\boldsymbol{\phi}_{\boldsymbol{n}}^{(d)} \tag{63}$$

and thus, decoupling the sum for each component of $\boldsymbol{n}$, it follows that

$$\begin{cases} E_h^{(1)} = \alpha_{\boldsymbol{0}}^{(1)}\displaystyle\sum_{n\in\mathbb{Z}} e^{ih\kappa_1 n}\chi_n(x_1)\sum_{n\in\mathbb{Z}} e^{ih\kappa_2 n}\theta_n(x_2) \\ E_h^{(2)} = \alpha_{\boldsymbol{0}}^{(2)}\displaystyle\sum_{n\in\mathbb{Z}} e^{ih\kappa_2 n}\chi_n(x_2)\sum_{n\in\mathbb{Z}} e^{ih\kappa_1 n}\theta_n(x_1) \end{cases} \tag{64}$$

It follows from (60) that

$$\sum_{n\in\mathbb{Z}} e^{ih\kappa n}\theta_n(s+nh) = e^{ih\kappa n}\sum_{n\in\mathbb{Z}} e^{ih\kappa n}\theta_n(s) \qquad \forall\, n\in\mathbb{Z} \tag{65}$$

Let $u\in H^1(\Omega)$ be an analytic solution of the homogeneous scalar Helmholtz equation in one dimension, defined by $u(s) = e^{i\kappa s}$. Consider V_h a finite element space. Note that equation (65) can be seen as a discrete version of u, i.e.,

$$u_h(\kappa, s) = \sum_{n\in\mathbb{Z}} e^{ih\kappa n}\theta_n(s) \tag{66}$$

Hence, the following variational problem can be considered: Find $u_h\in V_h$ such that

$$\left(\frac{du_h}{ds}, \frac{dv_h}{ds}\right)_{L_2} = \omega_h(\kappa)^2(u_h, v_h)_{L_2} \qquad \forall\, v_h\in\, V_h \tag{67}$$

or

$$\int_{\mathbb{R}} \frac{du_h}{ds}\frac{dv_h}{ds}\, ds = \omega_h(\kappa)^2\int_{\mathbb{R}} u_h v_h\, ds \qquad \forall\, v_h\in\, V_h \tag{68}$$

where $\omega_h(\kappa)^2$ can be calculated by replacing (66) in (68), by defining $v_h = \theta_m$, with $m \in \mathbb{Z}$, and by noting that $\theta_n(s)\theta_m(s) \neq 0$ just when $s \in (mh-h; mh+h)$. By taking the integral in each of the three plots($n = mh-h, mh, mh+h$), one has

$$\omega_h(\kappa)^2 = \frac{\sum_{n=(m-1)h}^{(m+1)h} e^{ih\kappa n} \int_{(m-1)h}^{(m+1)h} \theta_n'(s)\theta_m'(s)\, ds}{\sum_{n=(m-1)h}^{(m+1)h} e^{ih\kappa n} \int_{(m-1)h}^{(m+1)h} \theta_n(s)\theta_m(s)\, ds} \tag{69}$$

After solving the integrals and using the identity $2cos(\kappa h) = e^{ih\kappa} + e^{-ih\kappa}$, the following expression arises:

$$\omega_h(\kappa)^2 = \frac{6}{h^2}\frac{1-cos(h\kappa)}{2+cos(h\kappa)} \tag{70}$$

Furthermore, note that

$$\frac{du_h}{ds} = \left(\frac{e^{ih\kappa}-1}{h}\right) \sum_{n\in\mathbb{Z}} e^{ih\kappa n}\chi_n(s) \tag{71}$$

Equation (71) indicates that the function $\boldsymbol{E}_h$, defined in (64), can be expressed in the alternative form, given below

$$\begin{cases} E_h^{(1)} = \alpha_1 \dfrac{du_h(\kappa_1, x_1)}{dx_1} u_h(\kappa_2, x_2), \\ E_h^{(1)} = \alpha_2 \dfrac{du_h(\kappa_2, x_2)}{dx_2} u_h(\kappa_1, x_1) \end{cases} \tag{72}$$

where $\alpha_1 = \alpha_{\mathbf{0}}^{(1)}/i\kappa_1$ and $\alpha_2 = \alpha_{\mathbf{0}}^{(2)}/i\kappa_2$ with $h \longrightarrow 0$.
A non-trivial discrete solution of the form (72) is required, so as to satisfy the variational formulation presented in (49). Then, for all $\boldsymbol{n} \in \mathbb{Z}^2$, $\boldsymbol{v}_h \in \boldsymbol{V}_{h0}$ is chosen as

$$\boldsymbol{v}_h = \begin{bmatrix} \theta_{n_1}'(x_1)\theta_{n_2}(x_2) \\ 0 \end{bmatrix} \tag{73}$$

Using equation (72) combined with (68):

$$(\boldsymbol{E}_h, \boldsymbol{v}_h) = \omega_h(\kappa_1)^2 \alpha_1 \prod_{l=1}^{2} \int_{\mathbb{R}} u_h(\kappa_l; x_l)\theta_{nl}(x_l)\, dx_l \tag{74}$$

and

$$(\nabla \times \boldsymbol{E}_h, \nabla \times \boldsymbol{v}_h) = (\alpha_1 - \alpha_2)\omega_h^2(\kappa_1)\omega_h^2(\kappa_2)\prod_{l=1}^{2}\int_{\mathbb{R}} u_h(\kappa_l; x_l)\theta_{nl}(x_l)dx_l \tag{75}$$

Thus, equation (49) simplifies to the algebraic equation

$$\alpha_1\left(\omega_h(\kappa_2)^2 - \omega^2\right) - \alpha_2\omega_h(\kappa_2)^2 = 0 \tag{76}$$

Note that (76) remains the same, regardless the multi-index $\boldsymbol{n} \in \mathbb{Z}^2$. The same argument applies to the second component, i.e., by selecting

$$\boldsymbol{v}_h = \begin{bmatrix} 0 \\ \theta_{n_1}(x_1)\theta'_{n_2}(x_2) \end{bmatrix} \tag{77}$$

one has

$$\alpha_2\left(\omega_h(\kappa_1)^2 - \omega^2\right) - \alpha_1\omega_h(\kappa_1)^2 = 0$$

Therefore, equation (49) is reduced to a homogeneous system of two equations and two variables, α_1 e α_2. Consequently, the following equivalent condition for the existence of a non-trivial solution $\boldsymbol{E}_h$ is obtained:

$$\begin{vmatrix} -\omega^2 + \omega_h(\kappa_2)^2 & -\omega_h(\kappa_2)^2 \\ -\omega_h(\kappa_1)^2 & -\omega^2 + \omega_h(\kappa_1)^2 \end{vmatrix} = 0$$

or:

$$\omega^2 = \omega_h(\kappa_1)^2 + \omega_h(\kappa_2)^2 \tag{78}$$

Expression (78) is the discrete dispersion relation corresponding to the Whitney elements. By following the same steps, and making appropriate considerations to the degree p of the interpolation functions, an expression for the general case can be found; it reads:

$$\omega^2 = \omega_{hp}(\kappa_1)^2 + \omega_{hp}(\kappa_2)^2 \tag{79}$$

Using linear interpolants($p = 0$ order in the case of Whitney elements) in the discretization of the homogeneous Helmholtz equation, Babuška and Ihlenburg (1995), Thompson and Pinsky (1994) and Ainsworth (2003) demonstrated the following expression for relation discrete dispersion

$$cos(h\kappa) = \frac{6 - 2(h\omega_h(\kappa))^2}{6 + (h\omega_h(\kappa))^2} \qquad \text{with} \qquad h \longrightarrow 0 \tag{80}$$

which is the same equation (70), written in terms of $\omega_h(\kappa)$. Theorem 1 in Ainsworth (2003), shows how to build rational expressions for the cosine through Padé approximation, which are related to the order $q = p+1$ of the finite element method for the approximation of the Helmholtz equation. Such rational functions demonstrate better accuracy with the growth of the q-order used in interpolants of the discretized solution. In particular, for $p = 1$ (first-order Nédélec elements), the cosine rational expression is:

$$cos(h\kappa) = \frac{3(h\omega_h(\kappa))^4 - 104(h\omega_h(\kappa))^2 + 240}{(h\omega_h(\kappa))^4 + 16(h\omega_h(\kappa))^2 + 240} \qquad \text{with} \qquad h \longrightarrow 0 \tag{81}$$

The purpose of this section is to show how to select a mesh parameter h, which will make the difference in phase velocity, between the exact and approximate solution of the problem (47)-(48), become negligible. With this purpose, consider that the numerical phase velocity C is defined according to the p-order of the edge finite elemens used, as:

$$C = \frac{\omega_{hp}(\kappa)}{\kappa} \tag{82}$$

Note that equations (80) and (81) can be expressed in terms of $\omega_{hp}(\kappa)$, i.e.

$$\omega_{h0}(\kappa)^2 = \frac{6}{h^2}\left(\frac{1-cos(h\kappa)}{2+cos(h\kappa)}\right) \qquad (p=0) \tag{83}$$

and

$$\omega_{h1}(\kappa)^2 = \frac{1}{h^2}\left(\frac{16cos(h\kappa)+104+\sqrt{\alpha}}{6-2(cos(h\kappa))}\right) \qquad (p=1) \tag{84}$$

respectively, where $\alpha = (16cos(h\kappa)+104)^2 - 4(cos(h\kappa)-3)(cos(h\kappa)-1)$. Figure 6(a) depicts the comparison between the exact phase velocity $c = \omega/|\boldsymbol{\kappa}|$ of the continuous problem(consider $c = 1$, see equation (53)) and the numerical phase velocity when expressions (83) and (84), are substituted, in equation (82). Figure 6(b) depicts a closer view of Figure 6(a) that estimates, for example, the largest possible value of the parameter h so that the estimated phase error is less than 0.01%. To do so, simply observe the points where the velocity curves reach the value 1.0001, i.e., $\kappa h \approx 0,05$ and $\kappa h \approx 0,62$ for Whitney and Nédélec elements, respectively.

The estimates obtained for h are validated by means of the numerical experiments made in earlier section. By adapting use $\boldsymbol{\kappa} = (10\pi, 10\pi)$, then $\kappa_1 = \kappa_2 = 10\pi$, and thus the recommended values are: $h \approx \frac{0,05}{10\pi} \approx \frac{1}{629}$ (Whitney elements) and $h \approx \frac{0,62}{10\pi} \approx \frac{1}{51}$ (Nédélec elements).

In fact, for $h \leq \frac{1}{51}$ the phase difference in the experiment with Nédélec elements becomes negligible within the error suggested(0.01%). This shows that the dispersive effects caused by numerical approximation carried out with Whitney($p = 0$) and Nédélec($p = 1$) elements can be controlled according to the choice of initial parameter h estimated.

Equations (83) and (84) are employed to show the phase velocity approximation for a fixed κ and an increasing n. This is shown in Figures 7(a) and 7(b) for three different κ values. As expected, it is clear that improving the approximation for $c = 1$ requires smaller h values for larger frequency numbers, in a similar way followed by the approximate with edge finite element, see Figures 5(a) and 5(b). Therefore, we can characterize the error in the phase velocity can be characterized as error estimator in the edge finite element approximation.

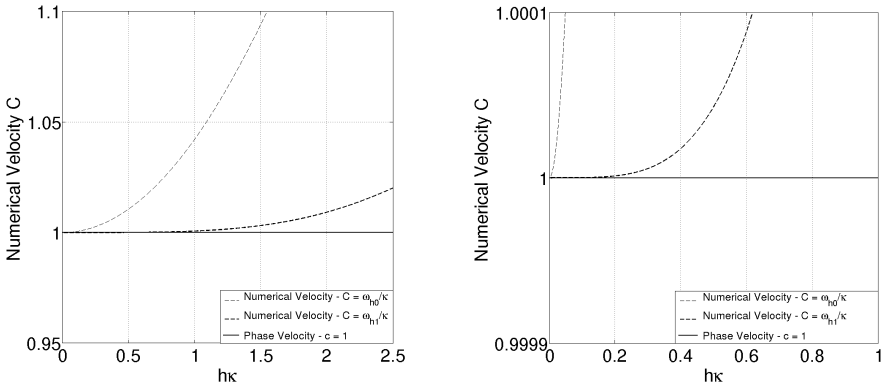

Figure 6: (a) Numerical phase velocity for Whitney and Nédélec elements, and phase velocity $c = 1$.; (b) Closer view Figure 6(a)

7 Conclusion

In this work the edge finite elements space of zero-order and first-order, known by Whitney elements and Nédélec elements, respectively, were described, furthermore, the hierachical basis function set to each finite element studied were built. A brief presentation of the second order time harmonic Maxwell system was also presented, together with some numerical experiments concerned with its solutions. Note that some interesting results in the approximation were found: The results revealed phase differences between the approximate and the exact solutions when

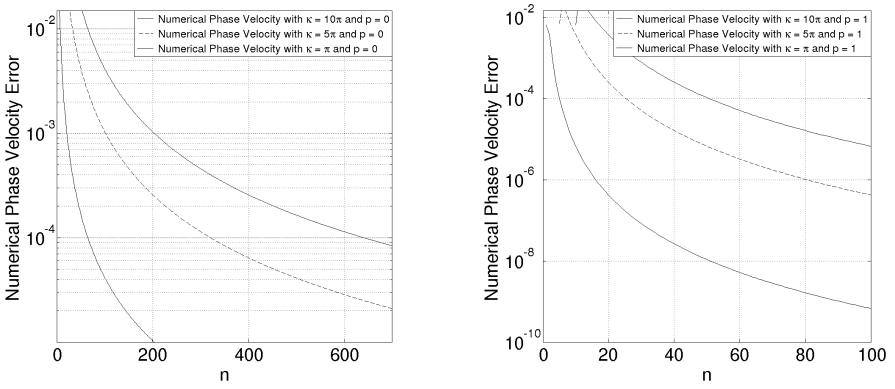

(a) (b)

Figure 7: (a) Error between the phase velocity of the continuous problem and the numerical phase velocity for Whitney elements; (b) Nédélec elements of first order. The number of elements in the mesh is given by n^2, where the mesh parameter is $h = 1/n$. (see Figure 2).

a fixed wave vector and a fixed temporal frequency. Another aspect that deserves attention is the presence of an amplitude difference when the frequency is changed. Two lemmas, which show a clear relationship between the scalar homogeneous Helmholtz equation and the second order time harmonic Maxwell system were presented, turning possible to adapt the dispersive effects, caused by finite element approximation of the Helmholtz equation, for the second order time harmonic Maxwell system approximation. The goal arises in the search of the proper mesh parameter, which provides quantitative information about the level of mesh refinement and necessary approximation in order to control the dispersive effects. For simplicity, this analysis was restricted to plane waves propagating with an angle of 45 degrees with the horizontal (as in the numerical experiments presented). Note that plane waves propagating in other directions presents no additional difficulties. Due to the numerical experiments it was observed that the error in the approximation by edge finite element have a strong correlation with the phase velocity error from the analyzed problem. This evidence suggests that the numerical phase velocity defined from the discrete relation dispersion can be used as an error estimator in the approximation of the second order time harmonic Maxwell system by edge finite element method.

References

Adjerid, S. (2002): Hierarchical finite element bases for triangular and tetrahedral elements. *Comput. Methods Appl. Mech. Engrg.*, vol. 190, pp. 2925–2941.

Ainsworth, M. (2003): Discrete dispersion for hp-version finite element approximation at high wavenumber. *SIAM J. Numer. Analysis*, vol. 42, pp. 553–575.

Ainsworth, M.; Coyle, J. (2001): Hierarchic hp-edge element families for Maxwell's equations on hybrid quadrilateral and triangular meshes. *Comput. Methods Appl. Mech. Engrg.*, vol. 190, pp. 6709–6733.

Babuška, I.; Ihlenburg, F. (1995): Dispersion analysis and error estimation of Galerkin finite element methods for the Helmholtz equation. *International Journal for Numerical Methods in Engineering*, vol. 38, pp. 3745–3774.

Boffi, D.; Perugia, I. (1999): Computation model of electromagnetic resonator: analysis of edge element approximation. *SIAM J. Numer. Ana.*, vol. 36, pp. 1264–1290.

Christon, M. (1999): The influence of the mass Matrix on the dispersive nature of the semi-discrete, second-order wave equation. *Methods Appl. Mech. Engrg.*, vol. 173, pp. 146–166.

Ciarlet, G. (1978): *The Element Method for Elliptic Problems*. North-Holland Pub, New York.

Colton, D.; Kress, R. (1983): *Integral Equations Methods in Scattering Theory*. John Wiley and Sons InC., New York.

Greenleaf, A. et al. (2007): Full-Wave Invisibility of Active Devices at All Frequencies. *Communications in Mathematical Physics*, vol. 275, pp. 749–789.

Harari, I. et al. (1996): Recent Developments in Finite Element Methods for Structural Acoustic. *Archives of Computational Methods in Engineering*, vol. 36, pp. 131–311.

Ihlenburg, F.; Babuška, I. (1997): Finite element solution of the Helmholtz equation with high wave number. *Society for Industrial and Applied Mathematics*, vol. 34, pp. 315–358.

Jackson, J. D. (1999): *Classical Electrodynamics*. John Wiley and Sons InC., Berkeley.

Jin, J. (2002): *The Finite Element Method in Electromagnetism Second Edition*. John Wiley and Sons InC., New York.

Kaplan, W. (1970): *Advanced Calculus*. House of Electronics Industry, New York.

Kreyszig, E. (1978): *Introductory Functional Analysis With Applications*. John Wiley and Sons, New York.

Macedo, A. (1988): *Eletromagnetismo*. Guanabara, Rio de Janeiro.

Monk, P. (1991): A finite element method for approximating the time-harmonic Maxwell equation. *Numerische Mathematik*, vol. 63, pp. 243–261.

Monk, P. (2003): A simple Proof of Convergence for an Edge Element Discretization of Maxwell Equations. *Lecture Notes in Computational Science and Engineering*, vol. 28, pp. 127–141.

Monk, P. (2003): *Finite Element Methods for Maxwell's Equations*. Oxford Science Publications, New York.

Monk, P.; Cohen, G. (1998): Gauss point mass lumping schemes for Maxwell equations. *Numerical Methods for PDEs*, vol. 14, pp. 63–88.

Monk, P.; Parrot, A. (1994): Dispersion analysis of finite element methods for Maxwell equations. *SIAM J. Sci. Comput.*, vol. 15, pp. 916–937.

Nédélec, J. (1980): Mixed finite elements in $\mathbb{R}^3$. *Numerische Mathematik*, vol. 35, pp. 315–341.

Nédélec, J. (1986): A new family of mixed finite elements in $\mathbb{R}^3$. *Numerische Mathematik*, vol. 50, pp. 57–81.

Olver, F. et al. (2010): *NIST - Handbook of mathematical functions*. Cambridge University Press, New York.

Reddy, B. (1986): *Funcional Analysis and Boundary-Value Problems: an Introductory Treatment*. John Wiley and Sons, New York.

Soares, D. et al. (2008): Numerical Computation of Electromagnetic Fields by the Time-Domain Boundary Element Method and the Complex Variable Method. *Computer Modeling in Engineering & Sciences*, vol. 25, no. 1, pp. 1–8.

Thompson, L.; Pinsky, P. (1994): Complex wavenumber Fourier analysis of the p-version finite element method. *Computat. Mech.*, vol. 13, pp. 255–275.

Whitney, H. (1957): *Geometry Integration Theory*. Princeton University Press., New Jersey.

Zhang, X. et al. (2014): Wave Propagation in Piezoelectric Rods with Rectangular Cross Sections. *Computer Modeling in Engineering & Sciences*, vol. 100, no. 1, pp. 1–17.